RKCL5080

CHARACTERIZATION OF Au-Rh/TiO$_2$ CATALYSTS BY CO ADSORPTION; XPS, FTIR AND TPD EXPERIMENTS

János Raskó[a,*], Ákos Koós[a], Kornélia Baán[b] and János Kiss[b]

[a] Reaction Kinetics Research Group of the Hungarian Academy of Sciences
at the University of Szeged

[b] Institute of Solid State and Radiochemistry, the University of Szeged, H-6701 Szeged,
P. O. Box 168, Hungary

Abstract

On X-ray photoelectron spectra of the Au-Rh/TiO$_2$ catalysts the position of Au4f peak was practically unaffected by the presence of rhodium, the peak position of Rh3d, however, shifted to lower binding energy with the increase of gold content of the catalysts. Rh enrichment in the outer layers of the bimetallic crystallites was experienced. The bands due to Au^0-CO, Rh^0-CO and (Rh^0)$_2$-CO were observed on the IR spectra of bimetallic samples, no signs for Rh$^+$-(CO)$_2$ were detected on these catalysts. The results were interpreted by electron donation from titania through gold to rhodium and by the higher particle size of bimetallic crystallites.

Keywords: TiO$_2$-supported Au-Rh bimetallic catalysts, XPS, FTIR

INTRODUCTION

The increasing demand for alternative energy sources initiated the catalytic research on hydrogen production either by the transformation of natural gas or from renewable base materials such as bioethanol [1,2]. Hydrogen produced by

* Corresponding author. Fax: +36-62-420-678; E-mail: rasko@chem.u-szeged.hu

either process always contains a significant amount of CO, the concentration of which (cca. 5-15 %) must be lowered to 1-100 ppm for the proper operation of a fuel cell producing energy with low environmental impact [3]. The most powerful process for the removal of CO proved to be the preferential oxidation (PROX) of CO. To find a proper catalyst for PROX process, however, is not a simple task. Although supported Au-based nanocatalysts show remarkable CO oxidation behavior at very low temperatures [4-7], the presence of hydrogen greatly suppressed their catalytic activity in CO oxidation [8].

Another approximation to overcome the problem caused by the relatively high concentration of CO in the fuel cell is to find a CO-tolerant H_2 oxidation catalyst, which works as an anode catalyst that oxidizes CO while maintains high activity for H_2 electrooxidation under 373 K. For this purpose Pt-Sn/C, Pt-Rh supported on MoO_3 and on TiO_2 [9] and γ-Al_2O_3-supported Au-Pt [10] bimetallic systems might be good candidates for low temperature CO-tolerant anode electrocatalysts. The main concern in the field of bimetallic catalysis is what happens if a mixture of two metals is deposited onto an inorganic oxide support forming thereby a highly dispersed catalyst [11]. Ponec [12] has listed some effects due to diminished particle size.

In this work attempts have been made to characterize the TiO_2-supported Au-Rh bimetallic catalysts by the adsorption of CO (as probe molecule), to study the possible electronic interaction between the two metallic components and between the support and the metallic part of the catalysts in order to elucidate the possible catalytic performance of these catalysts in CO oxidation and in the preferential oxidation of CO in the presence of hydrogen.

EXPERIMENTAL

Preparation of monometallic Au/TiO_2 and Rh/TiO_2 catalysts was described elsewhere [31, 32]. The bimetallic Au – Rh catalysts with three different compositions were produced by impregnating of TiO_2 (Degussa P25) with the mixtures of calculated volumes of $HAuCl_4$ (Fluka) and $RhCl_3 \times 3$ H_2O (Johnson Matthey) solutions to yield 1 wt.% metal content. The impregnated powders were dried in air at 383 K for 3 h. CO (99.97 %), and H_2 (99.999 %) were the products of Linde. The details of experimental setup and circumstances for infrared studies can be found elsewhere [8, 31, 32]. The adsorption and temperature programmed desorption (TPD) studies were carried out in a microbalance (Netzsch STA 409 PC) connected to a mass spectrometer (Pfeiffer QMS 200). Mass spectrometric analysis was performed with the help of a QMS 200 (Balzers) quadrupole mass-spectrometer. XP spectra were taken with a Kratos XSAM 800 instrument using non-monochromatic Mg $K\alpha$ radiation (hv = 1253.6 eV).

RESULTS AND DISCUSSION

After recording the X-ray photoelectron spectra of as-received samples in vacuum, the catalysts were reduced in the preparation chamber in H_2 for 1 h then H_2 was evacuated at 573 K; this was followed by cooling down to room temperature and transporting of the samples to the measuring chamber for obtaining the XP spectra of the reduced catalysts. Finally, the catalysts were contacted with CO (13.3 Pa) at 300 K for 15 min in the preparation chamber and after the evacuation of CO at 300 K, the XP spectra were recorded again. The positions of Ti2p and O1s peaks remained unaltered after the reduction of the catalysts. The peak position of Rh3d observed on the XP spectra of as-received samples shifted to lower binding energy after reduction. No appreciable change in the position of Au4f peak was recorded on the spectra of the reduced Au-containing samples in comparison with the as-received catalysts.
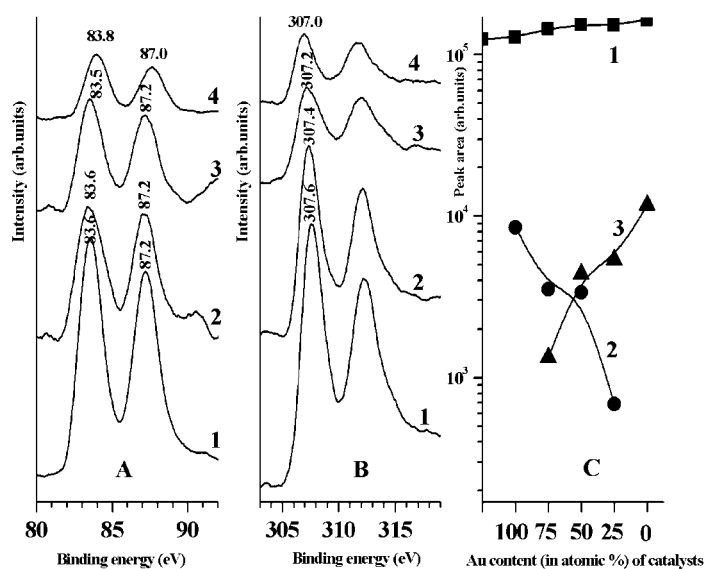

Fig. 1. (A) - Au4f region of XPS spectra of reduced catalysts; (B) - Rh3d region of XPS spectra of reduced catalysts (1 - 1 % Rh/TiO$_2$; 2 - 1 % (0.25Au+0.75Rh)/TiO$_2$; 3 - 1 % (0.5Au+0.5Rh)/TiO$_2$ and 4 - 1 % (0.75Au+0.25Rh)/TiO$_2$); (C) - XPS peak area of different components as a function of catalyst composition on the spectra of reduced catalysts (1 – Ti2p; 2 – Au4f and 3 – Rh3d)

The position of the Au4f peak did not change with the variation of Au:Rh ratio of the reduced catalysts (Fig. 1A). A continuous shift to the lower binding energy in the position of Rh3d peak of the reduced samples, however, can clearly be recognized (Fig. 1B) with the increase of the Au content of the catalysts. The changes of peak areas for Ti2p, Au4f and Rh3d of the reduced catalysts as a function of the catalyst composition are depicted on Fig. 1C. The peak area of Ti2p slightly increased with the increase of Rh content, while the peak areas of Au4f and Rh3d changed according to the nominal composition of the catalysts. Based on the peak area values corrected by the sensitivity factors the $Area_{Au}/Area_{Au}+Area_{Rh}$ and $Area_{Rh}/Area_{Au}+Area_{Rh}$ ratios were calculated (Table 1). The data clearly show that the outer layers contain more Rh than it could be expected from the nominal (bulk) composition of the catalysts. We did not observe further changes either in the peak positions, or in the peak areas after CO adsorption and evacuation at 300 K.
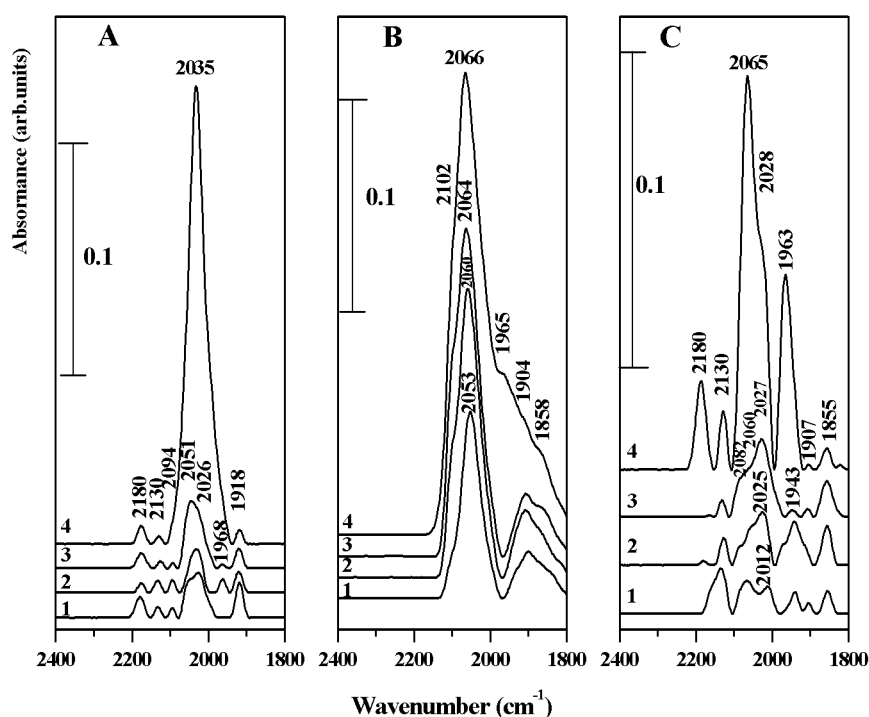

Fig. 2. IR spectra of reduced 1 % Au/TiO₂ (A), 1 % Rh/TiO₂ (B) and 1 % (0.5Au+0.5Rh)/TiO₂ (C) during CO adsorption at 300 K: 1 – 1.33 Pa; 2 – 13.3 Pa; 3 – 1.33 hPa and 4 – 13.3 hPa. Adsorption time 15 min

Besides the 2180 cm^{-1} band (CO adsorbed on TiO$_2$), bands at 2130, 2094, 2051, 2026, 1968 and 1918 cm^{-1} appeared in the range of 2400-1800 cm^{-1} during the low pressure (1.33 Pa-1.33 hPa) CO adsorption at 300 K on 1 wt.% Au/TiO$_2$ (Fig. 2A). With the increase of CO pressure to 1.33 hPa a shift from 2130 cm^{-1} to 2125 cm^{-1} was observed. In 13.3 hPa CO this band appeared at 2121 cm^{-1}. At the highest CO pressure applied here (13.3 hPa) one band with dramatically increased intensity at 2035 cm^{-1} appeared instead of the 2051 and 2026 cm^{-1} bands. The adsorption of 1.33 Pa CO on 1 wt.% Rh/TiO$_2$ caused the appearance of the bands at 2102, 2053, 1904 and 1858 cm^{-1} (Fig. 2B). With the increase of CO pressure the 2053 cm^{-1} band shifted to higher wavenumbers; in 13.3 hPa CO this band was observed at 2066 cm^{-1} and a new band at 1965 cm^{-1} appeared. Due to the evacuation at 300 K for 15 min the intensities of the bands slightly diminished and the band at 2066 cm^{-1} (observed in the presence of CO) shifted to 2055 cm^{-1}. The spectra due to CO adsorbed at 300 K on 1 wt.% (50 atomic % Au+50 atomic % Rh)/TiO$_2$ sample illustrate what happened on the surfaces of bimetallic catalysts during CO adsorption (Fig. 2C). Bands due to CO adsorbed on Au-sites and on Rh-centres, respectively, can be distinguished even under the lowest CO pressure. The most striking change is observed in the position of the band around 2020 cm^{-1}, which belongs to an Au-CO species. This band appeared at 2012 cm^{-1} in 1.33 Pa CO, its position shifted to higher wavenumbers with the increase of CO pressure. In 13.3 hPa CO it was observed at 2028 cm^{-1}. After a short evacuation at 300 K the intensity of all bands greatly reduced, the band that appeared at 2065 cm^{-1} in CO shifted to 2050 cm^{-1} and a new band at 2090 cm^{-1} (probably overlapped by the intense 2065 cm^{-1} band in CO) became clearly observable. Similar features were detected on other bimetallic catalysts; the intensity of the bands due to Rh-CO species evidently increased with the increase of Rh-content.

For proper comparison the spectra in 13.3 hPa CO after 60 min of adsorption at 300 K were depicted on Fig. 3. It is to be noted that the adsorption capacity of the bimetallic catalysts was smaller than that of monometallic Au/TiO$_2$ and Rh/TiO$_2$ catalysts (see multiplication factors on the spectra of bimetallic catalysts). It can be noticed that bands due to Rh-CO species (2066, 1965 and 1860 cm^{-1}) were dominant in the spectra of bimetallic catalysts. CO uptake was the highest on monometallic catalysts (on 1% Au/TiO$_2$: 4.3 mg/g cat and on 1% Rh/TiO$_2$: 5.2 mg/g cat). The amounts of CO bonded to the surfaces of the bimetallic catalysts were substantially lower (1.1 – 3.1 mg/gcat). After the He-purge of the system at 300 K no CO desorption from Au/TiO$_2$ and bimetallic catalysts was observed in the TPD experiments.

Although the number of works on bimetallic catalysis has significantly grown in the last decades, no generally accepted theory concerning the catalytic effects of bimetallic catalysts can be found in the literature. It turned out in the very early stage of the studies that the models built up for the non-supported

bimetallic systems (such as rigid band model [13]), formation of alloy [14-17], surface enrichment in the component with lower heat of sublimation [18], "cherry model" [19], coherent potential approximation [16, 17], ensemble and ligand effect [18-22] and electron transfer [23, 24]) cannot be simply transformed to the supported bimetallic catalysts. UPS studies [25, 26] revealed that metal crystallites having more than 150 atoms behave like a bulk metal. At lower particle sizes (ca. 50 metal atoms) the electronic structure is altered. Alloy formation can also be predictable in most cases of supported bimetallic catalysts, which can be influenced by the nature of the catalyst carrier [27-30]. The supporting oxide in our study was TiO_2, the reduction of which above 623 K would lead to strong metal support interaction (SMSI); this phenomenon may further strongly influence the electronic properties of the bimetallic particles. The reduction temperature (573 K) applied here hindered the occurrence of SMSI, thus this effect can be disregarded.

Our recent data on acetonitrile adsorption on Au/TiO_2 [31], Rh/TiO_2 [32] and $Au-Rh/TiO_2$ [33] catalysts revealed an electron interaction between TiO_2 and the metallic particles: the electron flow is directed from TiO_2 to the metal. As a consequence of this electron donation the formation of strong Lewis acid sites on titania has been established on Au/TiO_2 and Rh/TiO_2. An interesting finding was that the strength of Lewis acid sites weakened with the increase of Rh content in bimetallic Au – Rh catalysts [33], which predicts a special electronic interaction between the two metals. The present XPS results show that after the reduction of monometallic catalysts, the corresponding metal is very near to its most reduced state: the peak position of Au4f was 83.6 eV, that of Rh3d was 307.6 eV on 1% Au/TiO_2 and 1% Rh/TiO_2, respectively. The peak position of the bulk metals are: 83.8 eV (Au4f) and 307.0 eV (Rh3d) [34]. With the increase of the Rh content the XPS peak position of Au4f remained practically constant (Fig. 1A), while that of Rh3d shifted to lower binding energy with the increase of Au content of the catalysts (Fig. 1B). The possible electron donation between the components of the catalysts is governed by the work function value ($\Delta\varphi$) of the individual parts of the samples. The work function of reduced TiO_2 is 4.8 eV (35), that for polycrystalline Au is 5.38 eV [36] and ($\Delta\varphi$) of polycrystalline Rh is 4.98 eV [37]. On the basis of these literature data the most electron donating component should be TiO_2, the most electron accepting part of our catalysts has to be gold. According to the picture obtained in the present XPS study, however, Rh seems to be the most electron accepting component of the $Au-Rh-TiO_2$ catalysts, as only its characteristic 3d peak shifted to lower binding energy with the increase of gold content. We suppose that the electron donation from TiO_2 to gold and gold – in spite of the ($\Delta\varphi$) values – conveyed the electrons to Rh. This is probably due to the filled d – orbital of gold and the difference in binding energy between Au4f and Rh3d orbitals.

Table 1

Composition of the outer layers of the reduced catalysts based on XPS data

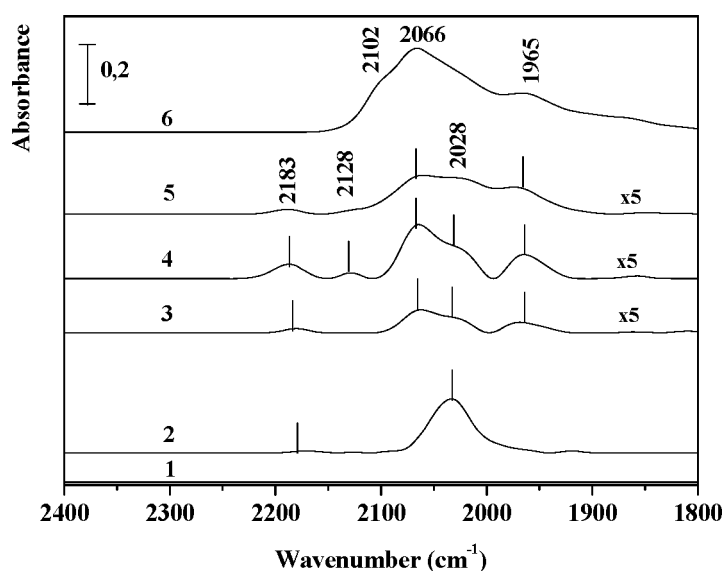| Nominal composition	$Area_{Au}/Area_{Au}+Area_{Rh}$	$Area_{Rh}/Area_{Au}+Area_{Rh}$
1 % Au/TiO$_2$	1.00	0.00
1 % (0.75Au+0.25Rh)/TiO$_2$	0.69	0.31
1 % (0.50Au+0.50Rh)/TiO$_2$	0.39	0.61
1 % (0.25Au+0.75Rh)/TiO$_2$	0.10	0.90
1 % Rh/TiO$_2$	0.00	1.00

Fig. 3. IR spectra of reduced catalysts registered at 300 K in 13.3 hPa CO after 60 min adsorption time: 1 – TiO$_2$; 2 – 1% Au/TiO$_2$; 3 – 1% (0.75Au+0.25Rh)/TiO$_2$; 4 – 1% (0.5Au+0.5Rh)/TiO$_2$; 5 – 1% (0.25Au+0.75Rh)/TiO$_2$ and 6 –1% Rh/TiO$_2$

From the experimental findings (Rh enrichment in the outer layers (Table 1), lower capacity for CO adsorption of bimetallic catalysts) we intend to think that particles containing both Au and Rh atoms formed on the titania surface and the size of these bimetallic particles is greater than the particle size of monometallic catalysts. The intensity values of the bands due to adsorbed CO (Fig. 3) point

out that the number of the adsorption sites greatly reduced by the presence of the second metal. Similarly to the former results [38-40] the band at 2066 cm^{-1} (CO adsorbed linearly to Rh^0) at 1965 cm^{-1} (bridged bonded CO, Rh$^0_2$CO) and at 2102 cm^{-1} (symmetric stretching of Rh$^+$(CO)$_2$) appeared on the spectrum of reduced 1% Rh/TiO$_2$. Band due to the asymmetric stretching of Rh$^+$(CO)$_2$ around 2030 cm^{-1} was overlapped by the broad 2066 cm^{-1} band. In the cases of bimetallic Au–Rh samples, however, no signs for Rh$^+$(CO)$_2$ species (the presence of Rh$^+$ adsorption sites) were observed on the IR spectra. This can be regarded as a further proof of electron donation from gold to rhodium in the bimetallic particles, which keeps Rh in reduced state.

CONCLUSIONS

1. Electron donation from TiO$_2$ through Au to Rh occurs in TiO$_2$-supported bimetallic catalysts.
2. Rh enrichment in the outer layers of bimetallic particles was observed.
3. Adsorptive capacity of bimetallic catalysts was lower than that of monometallic samples, possibly due to the higher particle size in bimetallic crystallites.
4. The behavior of CO adsorbed on gold was not affected by the presence of rhodium.

REFERENCES

1. J.N. Armor: *Appl. Catal.*, **176**, 159 (1999).
2. F. Aupretre, C. Descorme, D. Duprez: *Catal. Commun.*, **3**, 263 (2002).
3. A.J. Appleby, F.R. Foulkes: *Fuel Cell Handbook*. Van Nostrand Reinhold, New York, 1989.
4. M. Haruta, T. Kobayashi, S. Iijama, F. Delannay: *Proc. 9th Int. Congr. Catal.*, **3**, 1206 (1988).
5. D. Cunningham, S. Tsubota, N. Kamijo, M. Haruta: *Res. Chem. Intermed.*, **19**, 1 (1993).
6. M.A. Bollinger, M.A. Vannice: Appl. Catal. B: *Environmental*, **8**, 417 (1996).
7. S. Lin, M.A. Bollinger, M.A. Vannice: *Catal. Lett.*, **17**, 245 (1993).
8. J. Raskó, J. Kiss: *Catal. Lett.*, **111**, 87 (2006).
9. G. Avgouropoulus, T. Ioannides: Appl. Catal.B: *Environmental*, **56**, 77 (2005).
10. S. Zhou. K. McIlwrath, G. Jackson, B. Eichhorn: *J. Am. Chem. Soc.*, **126**, 1780 (2006).
11. L. Guczi: *Catal. Today*, **101**, 53 (2005).

12. V. Ponec: *Adv. Catal.*, **32**, 149 (1983).
13. D.A. Dowden, P.W. Reynolds: *Discuss. Faraday Soc.*, **8**, 184 (1950).
14. D.F. Ollis: *J. Catal.*, **23**, 131 (1971).
15. W.H.M. Sachtler: in R. Prins, G.C. Schuit (Eds.): *Chemistry and Chemical Engineering of Catalysis Processes*, p. 317. Sijthoff and Noordhoff, The Netherlands, 1980.
16. V. Ponec, G.C. Bond (Eds.): Catalysis by Alloys. Elsevier, Amsterdam 1995.
17. L. Guczi, A Sárkány: *Catalysis*, in: J.J. Spivey (Ed.), Special Periodical Reports, Vol. 11. Chapter 8, p. 318. The Chemical Society, London 1994.
18. W.H.M. Sachtler, R.A. van Santen: *Adv. Catal.*, **26**, 69 (1977).
19. W.H.M. Sachtler, R.A. van Santen: *Appl. Surf. Sci.*, **3**, 121 (1979).
20. J.H. Sinfelt: *Acc. Chem. Res.*, **10**, 15 (1977).
21. J.K.A. Clarke: *Chem. Rev.*, **75**, 291 (1975).
22. V. Ponec, in: E.G. Derouane, A.A. Lucas (Eds.), *Electronic Structure and Reactivity of Solid Surfaces*, p. 537. Plenum Press, New York 1976.
23. U. Bardi, A. Atrei, P. Ross, E. Zanazzi, G. Rovida: *Surf. Sci.*, **211-212**, 441 (1989).
24. J.W. He, D.W. Goodman: *J. Phys. Chem.*, **94**, 1502 (1999).
25. R.C. Baetzold: *Surf. Sci.*, **106**, 243 (1981).
26. R.C. Baetzold, J. Hamilton: *Progress in Solid State Chemistry*, Vol. 15. Pergamon Press, p. 1. New York 1983.
27. N. Wagstaff, R. Prins: *J. Catal.*, **59**, 434 (1979).
28. P.S. Kirlin, B.R. Strochmeier, B.C. Gates: *J. Catal.*, **98**, 308 (1986).
29. H. Topsoe, J.A. Dumesic, E.G. Derouane, B.S. Clause, S. Morup, J. Villadsen, N. Topsoe in: B. Delmon et al. (Eds.): Preparation of Catalysts, Vol. 2, p. 365. Elsevier, Amsterdam 1979.
30. P. Turliers, J.A. Dalmon, G.A. Martin: in: B. Imelik et al. (Eds.), *Metal Support and Metal Additives Effects in Catalysis*, p. 203. Elsevier, Amsterdam 1983.
31. J. Raskó, J. Kiss: *Catal. Lett.*, **109**, 71 (2006).
32. J. Raskó, J. Kiss: *Appl. Catal. A: General*, **303**, 56 (2006).
33. J. Raskó, J. Kiss, to be published.
34. C.D. Wagner, W.M. Riggs, L.E. Davis, J.F. Moulder, G.E. Muilenberg: Handbook of X-Ray Photoelectron Spectroscopy. Perkin-Elmer Co. 1978.
35. Y.W. Chung, W. Lo, G.A. Somorjai: *Surf. Sci.*, **64**, 588 (1977).
36. M. Uda, A. Nakamura, T. Yamamoto, Y. Fujimoto: *J. Electr. Spectr.*, **88-91**, 643 (1998).
37. CRC Handbook of Chemistry and Physics. CRC Press, Boca Raton FL 1979.
38. F. Solymosi, M. Pásztor: *J. Phys. Chem.*, **89**, 4783 (1985).
39. M. Primet: *J. Chem. Soc. Faraday Trans.*, **74**, 2570 (1978).
40. C.A. Rice, S.D. Worley, C.W. Curtis, J.A. Guin, A.R. Tarrer: *J. Chem. Phys.*, **74**, 6748 (1981).